CHARGE-PRODUCT CONTROL APPROACH TO ELECTROSTATIC LEADER-FOLLOWER IN LEO PLASMA WAKES

Jordan Maxwell * **and Hanspeter Schaub** †

A novel method for close-proximity formation flying under differential atmospheric drag using Coulomb forces is investigated for applications in Earth sensing, space-situational awareness (SSA), and aeronomy. Objects in LEO are supersonic with respect to the ambient environment, creating a thinned out wake region antiparallel to the craft's atmosphere-relative velocity. Objects within this wake experience little drag acceleration and are able to attain voltages much greater than in the ambient ionospheric plasma, creating implications for the design and control of close-proximity leader-follower spacecraft pairs. The proposed system consists of a leader craft with a set of affixed, conducting spheres and a charged follower craft located in the wake of the leader. A deployment scenario is considered in which a controlled Coulomb repulsion guides the follower along a proscribed trajectory to its nominal position. A charge-product control vector is chosen for simplicity and a asymptotically stabilizing kinematic steering law is derived using Lyapunov's Direct Method. Simulations are run under unmodeled perturbations to demonstrate the control method's effectiveness.

INTRODUCTION

The desire for enhanced space-based infrastructure coupled with the costs and challenges of launching spacecraft into orbit necessitates precise, fuel efficient relative motion control technologies. Conventional techniques match the plane of a two craft — chaser and target — achieve proper phasing and orbit radius, and correct attitude rates using thrusters.[1] The increased risk of collision associated with close-proximity operations demands that translational and rotational states are controlled to high precision, requiring more fuel. High precision control is difficult to achieve with chemical thrusters due to their minimum turn-on thrust, which is typically larger than required when near the nominal state. Electric thrusters often lack the authority to overcome environmental perturbations on relevant timescales. Therefore, a technology with high resolution and dynamic range is desirable. This paper considers the use of a technique called electrostatic actuation for accomplishing rendezvous operations after two craft are in close proximity.

Electrostatic actuation[2] utilizes surface charge on close-proximity craft to generate relative translational and rotational accelerations. The key benefit are its touchless nature and use of renewable resources, namely spacecraft power. Additionally, the technique has high control resolution because a large change in craft voltage — relative to typical power system resolutions — generates a small acceleration. High dynamic range can be achieved given careful system design. As the control authority drops off as $1/r^2$, the technique is supplemental to conventional thrusters which will place the chaser in close proximity to the target. The fuel savings and high-precision control offered by the technique facilitate the final stages of the rendezvous.

GEO applications for electrostatic actuation have previously been the primary research focus because the plasma in this region is hot and sparse — prime conditions for charging and electrostatic force and torque

*Graduate Research Assistant, Department of Aerospace Engineering Sciences, University of Colorado, 431 UCB, Colorado Center for Astrodynamics Research, Boulder, CO 80309-0431

†Glenn L. Murphy Endowed Chair, Department of Aerospace Engineering Sciences, University of Colorado, 431 UCB, Colorado Center for Astrodynamics Research, Boulder, CO 80309-0431

propagation. The electrostatic tractor technique[3] employs an electron/ion beam to charge another orbiting body, generating electrostatic forces and torques for touchless interactions to accomplish space debris removal,[4,5] detumbling of rapidly rotating objects on orbit,[3] orbital corrections,[6] and electrostatically inflated gossamer structures.[7] This paper represents the first investigation of the use of electrostatic actuation to facilitate rendezvous operations between two cooperative craft.

Low Earth Orbit (LEO) applications have until recently been dismissed because the cold, dense plasma in that regime shields electrostatic fields. However, the plasma wake which form naturally behind objects in LEO exhibits plasma parameters more amenable to the technique. Wakes form behind orbiting objects in LEO because the orbital velocity is supersonic with respect to the plasma ions and neutrals. This creates a region antiparallel to the object's velocity that is nearly devoid of these species.[8] Electrons, which have extremely low mass, move much more rapidly and are therefore able to penetrate into the wake. However, the lack of ions in this region creates a negative space charge which screens out lower-energy electrons, so the electron density is decreased and the temperature increased relative to ambient. This facilitates electrostatic actuation, as these conditions allow for enhanced electric field propagation.

A challenge of using electrostatic actuation in the wake is the plasma dynamics resulting from large vehicle voltages. Therefore, careful system design is required in which the target craft generates a wake much larger than the chaser. It has been shown that wake of the target craft can be expanded via surface charging to allow for a greater working volume and larger voltages for electrostatic actuation.[?,?] The use of voltage control based linear-quadratic regulator application of electrostatic actuation for deployment and precise control of a follower craft from a leader has been investigated,[?] but the nonlinearities inherent in the technique proved prohibitive. Instead, a charge-product based control methodology[?] is adopted in this paper. This approach simplifies the control development significantly, though a nonlinear control methodology is applied.

This paper first defines the specifics of the problem being investigated. Nonlinear equations of motion for the relative Coulomb, drag and gravity accelerations are then derived. A control development applying Lyapunov Direct Method is presented. Finally, results are shown and discussed before final conclusions are presented.

Problem Statement

A rendezvous scenario is considered in which a chaser craft is placed into a close-proximity leader-follower configuration with the target. The leader is assumed to have a set of conducting spheres in a circular pattern which can be charged to control the follower — modeled as a single conducting sphere — to a nominal position displaced slightly from the leader. Figure 1 depicts the configuration.

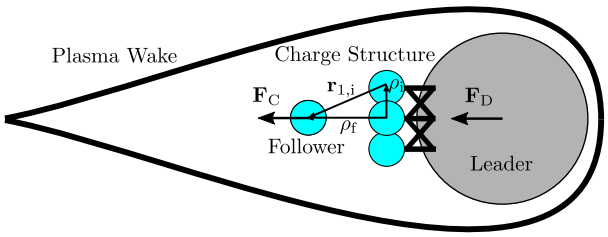

Figure 1. Illustration of desired rendezvous configuration

The follower is assumed to remain within the wake of the leader at all times. When the nominal position is achieved, a balance of differential drag and Coulomb repulsion is used to hold the follower in this location. For this investigation, it is assumed that no atmospheric density in the wake. While this is likely not the case, neutral flows in the wake are complicated and the effectiveness of the control can still be assessed using this simple model.

NONLINEAR EQUATIONS OF MOTION

Three perturbations are included in the simplified model used throughout this investigation: Two-body gravity, orbital drag, and Coulomb forces. The Hill-Clohessy-Whiltshire (HCW) frame is used with the origin at the center of the charge structure attached to the leader. The relative equations of motion are therefore

$$\ddot{\boldsymbol{\rho}} = \boldsymbol{\delta a}_{\mathrm{C}} + \boldsymbol{\delta a}_{\mathrm{D}} + \boldsymbol{\delta a}_{\mathrm{G}} \tag{1}$$

where $\ddot{\boldsymbol{\rho}} = \ddot{\boldsymbol{r}}_{\mathrm{f}} - \ddot{\boldsymbol{r}}_{\mathrm{l}}$ represents the total acceleration of the follower relative to the leader and $\boldsymbol{\delta a}_i$ the acceleration of the follower relative to the leader generated by the i^{th} perturbation. Note that the dot notation is used to represent an inertial derivative (i.e. $\dot{\boldsymbol{x}} \equiv \overset{\mathcal{N}}{\frac{\mathrm{d}}{\mathrm{d}t}}\boldsymbol{x}$).

Relative Drag and Gravitational Accelerations

The commonly used expressions for atmospheric drag and gravitational inertial accelerations are presented below.

$$\ddot{\boldsymbol{a}}_{\mathrm{D}} = -\frac{1}{2}\frac{AC_{\mathrm{D}}\gamma v_r}{m}\boldsymbol{v}_r \tag{2}$$

$$\ddot{\boldsymbol{a}}_{\mathrm{G}} = -\frac{\mu}{r^3}\boldsymbol{r} \tag{3}$$

Here, A is the cross-sectional area of a craft, C_{D} its drag coefficient, m its mass, and $\boldsymbol{v}_r$ its atmosphere-relative velocity; γ is the atmospheric density; and μ is the gravitational parameter of Earth. Writing these in terms of the relative accelerations of a leader and follower yields

$$\boldsymbol{\delta a}_{\mathrm{D}} = \frac{1}{2}\left(\frac{A_{\mathrm{f}}C_{\mathrm{D_f}}\gamma_{\mathrm{f}}}{m_{\mathrm{f}}} - \frac{A_{\mathrm{l}}C_{\mathrm{D_l}}\gamma_{\mathrm{l}}}{m_{\mathrm{l}}}\right) v_r\boldsymbol{v}_r \tag{4}$$

$$\boldsymbol{\delta a}_{\mathrm{G}} = \mu\left(\frac{\boldsymbol{r}_{\mathrm{f}}}{r_{\mathrm{f}}^3} - \frac{\boldsymbol{r}_{\mathrm{l}}}{r_{\mathrm{l}}^3}\right) \tag{5}$$

Note above that it is assumed that the atmosphere-relative velocities are identical between the two craft. Given that the differences in area, mass, drag coefficient, and local density dominate the differential drag term for such close-proximity craft, this is a reasonable assumption. A similar assumption that $\boldsymbol{r}_{\mathrm{f}} = \boldsymbol{r}_{\mathrm{l}}$ cannot be made in the gravity case, as differential gravitational accelerations arise only from the difference in these positions.

Relative Coulomb Acceleration

The Coulomb force between the follower and leader is calculated from the charge on the follower (Q_{f}) and the electric field of the leader ($\boldsymbol{E}_{\mathrm{L}}$).

$$\boldsymbol{F}_{\mathrm{C}} = Q_{\mathrm{f}}\boldsymbol{E}_{\mathrm{L}} \tag{6}$$

The proximity of the follower to the charge structure on the leader means that a mutual capacitance exists between the two objects. This affect is described by the relation between the voltage and the charge on a given object.

$$V_i = k_{\mathrm{C}}\frac{Q_i}{R_i} + k_{\mathrm{C}}\sum_{j=1,j\neq i}^{n}\frac{Q_j}{r_{i,j}} \tag{7}$$

Here, $k_{\mathrm{C}} = 8.99 \times 10^9$ Nm^2/C^2 is Coulomb's constant, R_i is the radius of the i^{th} sphere, and $r_{i,j}$ is the distance between the i^{th} and j^{th} spheres. Throughout this paper, the subscript 1 refers to the follower and subscripts 2 through n refer to the spheres on the leader's charge structure. The relation above can be rewritten

into a single matrix equation.

$$\begin{pmatrix} V_1 \\ V_2 \\ \vdots \\ V_n \end{pmatrix} = k_{\mathrm{C}} \begin{bmatrix} {}^{1}\!/_{R_1} & {}^{1}\!/_{r_{1,2}} & \dots & {}^{1}\!/_{r_{1,n}} \\ {}^{1}\!/_{r_{2,1}} & {}^{1}\!/_{R_2} & \dots & {}^{2}\!/_{r_{2,n}} \\ \vdots & \vdots & \ddots & \vdots \\ {}^{1}\!/_{r_{n,1}} & {}^{1}\!/_{r_{n,2}} & \dots & {}^{1}\!/_{R_n} \end{bmatrix} \begin{pmatrix} Q_1 \\ Q_2 \\ \vdots \\ Q_n \end{pmatrix} \tag{8}$$

Written in a more compact fashion

$$\boldsymbol{V} = [S]\boldsymbol{Q} \tag{9}$$

where $[S]$ is the elastance matrix.[9] Another well-known expression relating charge to voltage, $\mathbf{Q} = [C]\mathbf{V}$ indicates that the capacitance is the inverse of the elastance matrix.

$$\mathbf{Q} = [S]^{-1}\mathbf{V} \tag{10}$$

The electric field of the leader is the superposition of the individual fields from the charged spheres on the leader craft.

$$\boldsymbol{E}_{\mathrm{L}} = k_{\mathrm{C}} \sum_{i=2}^{n} \frac{Q_i}{r_{1,i}^3} \boldsymbol{r}_{1,i} \tag{11}$$

Here, $\boldsymbol{r}_{1,i}$ is a vector pointing from the i^{th} sphere to the follower craft. The collection of charged spheres on the leader create electrostatic potential well like that shown in Figure **??** according to this equation. Combining with Eq. (6) yields the force of the follower in terms of only the distance between the follower and each sphere and the charges. Henceforth, the follower craft is indicated by the numeral 1 to indicate its position within Eq. (8).

$$\boldsymbol{F}_{\mathrm{C}} = k_{\mathrm{C}} Q_1 \sum_{i=2}^{n} \frac{Q_i}{r_{1,i}^3} \boldsymbol{r}_{1,i} \tag{12}$$

This equation can also be interpreted in terms of a superposition of the Coulomb force generated between the follower and each of the charged spheres on the leader. Since a charge-product control methodology is applied within this investigation. Eq. (12) is rewritten in matrix-vector form and in terms of the control vector $\boldsymbol{u} = [Q_1Q_2, Q_1Q_3, ..., Q_1Q_n]^T$ below.

$$\boldsymbol{F}_{\mathrm{C}} = k_{\mathrm{C}}[R]\boldsymbol{u} \tag{13}$$

where $[R] = [{}^{\boldsymbol{r}_{1,2}}\!/_{r_{1,2}^3}, {}^{\boldsymbol{r}_{1,3}}\!/_{r_{1,3}^3}, ..., {}^{\boldsymbol{r}_{1,n}}\!/_{r_{1,n}^3}]$.

Finally, the relative Coulomb acceleration is written, recalling that the force on each craft is equal and opposite. Below, the control effect matrix $[B]$ is defined.

$$\boldsymbol{\delta a}_{\mathrm{C}} = \frac{1}{m_{\mathrm{f}}} \boldsymbol{F}_{\mathrm{C_f}} - \frac{1}{m_{\mathrm{l}}} \boldsymbol{F}_{\mathrm{C_l}} = -k_{\mathrm{C}} \left(\frac{m_{\mathrm{f}} + m_{\mathrm{l}}}{m_{\mathrm{f}} m_{\mathrm{l}}} \right) [R]\boldsymbol{u} = [B]\boldsymbol{u} \tag{14}$$

CONTROL METHODOLOGY

A control approach similar to that described in reference 10 is applied to the scenario described previously. The control is derived in terms of leader-relative vectors, as the relative dynamics between the leader and follower are relevant to the DPCA mission. A candidate Lyapunov function is proposed.

$$V_1 = \frac{1}{2} \boldsymbol{\delta\rho}^T \dot{\boldsymbol{\delta\rho}} \tag{15}$$

Here, $\boldsymbol{\delta\rho} = \boldsymbol{\rho} - \boldsymbol{\rho}_r$ is the difference between the current leader-relative position of the follower and the reference trajectory. The derivative of this candidate function is taken below. Since $\dot{V}_1$ must be negative

definite for the system to be asymptotically stable, the leader-relative velocity is set equal to $-\boldsymbol{f}(\boldsymbol{\delta\rho})$. In order for $\dot{V}_1$ to be negative definite under this replacement, $\boldsymbol{f}(\boldsymbol{\delta\rho})$ is constrained to be an odd function.

$$\dot{V}_1 = \boldsymbol{\delta\rho}^T \dot{\boldsymbol{\delta\rho}} = -\boldsymbol{\delta\rho}^T \boldsymbol{f}(\boldsymbol{\delta\rho}) \tag{16}$$

Due to the possibility of collapsing the wake if overly large voltages are sourced, a control that saturates under large position differences is desired. A candidate function with this property is presented.

$$f_i(\boldsymbol{\delta\rho}) = \tan^{-1}\left(\delta\rho_i \frac{K\pi}{2\dot{\delta\rho}_{\max}}\right)\frac{2\dot{\delta\rho}_{\max}}{\pi} \tag{17}$$

In order to constrain the leader-relative velocity to adhere to the equation above, an outer control loop must be derived which controls the accelerations. Consider the candidate Lyapunov function below as well as its derivative.

$$V_2 = \frac{1}{2}\dot{\boldsymbol{\Delta\rho}}^T \dot{\boldsymbol{\Delta\rho}} \tag{18}$$

$$\dot{V}_2 = \dot{\boldsymbol{\Delta\rho}}^T \ddot{\boldsymbol{\Delta\rho}} \tag{19}$$

The quantity $\dot{\boldsymbol{\Delta\rho}} = \dot{\boldsymbol{\delta\rho}} - \dot{\boldsymbol{\delta\rho}}^*$ represents the difference between the actual velocity deviation from the reference trajectory and that desired. The combination of the position and velocity control loops is realized by setting $\dot{\boldsymbol{\delta\rho}}^* = \boldsymbol{f}(\boldsymbol{\delta\rho})$. Given this definition, the derivative of $\dot{\boldsymbol{\Delta\rho}}$ is calculated.

$$\ddot{\boldsymbol{\Delta\rho}} = \boldsymbol{\delta a}_{\mathrm{C}} + \boldsymbol{\delta a}_{\mathrm{D}} + \boldsymbol{\delta a}_{\mathrm{G}} - \ddot{\boldsymbol{\rho}}_{\mathrm{r}} + \dot{\boldsymbol{f}}(\boldsymbol{\delta\rho}, \dot{\boldsymbol{\delta\rho}}) \tag{20}$$

The reference trajectory is later defined in the HCW frame for simplicity, so its inertial derivative is computed in terms of its HCW-frame derivatives (denoted by primes rather than dots) and the rotating-frame accelerations.

$$\ddot{\boldsymbol{\rho}}_{\mathrm{r}} = \boldsymbol{\rho}_{\mathrm{r}}'' + \dot{\boldsymbol{\omega}}_{\mathcal{H}/\mathcal{N}} \times \boldsymbol{\rho}_{\mathrm{r}} + 2\boldsymbol{\omega}_{\mathcal{H}/\mathcal{N}} \times \boldsymbol{\rho}_{\mathrm{r}}' + \boldsymbol{\omega}_{\mathcal{H}/\mathcal{N}} \times \boldsymbol{\omega}_{\mathcal{H}/\mathcal{N}} \times \boldsymbol{\rho}_{\mathrm{r}} \tag{21}$$

Finally, the derivative of the outer-loop saturating control function is presented.

$$\dot{f}_i(\boldsymbol{\delta\rho}, \dot{\boldsymbol{\delta\rho}}) = \frac{K\dot{\delta\rho}_i}{1 + \left(\delta\rho_i \frac{K\pi}{2\delta\rho_{\max}}\right)} \tag{22}$$

In order to obtain a globally asymptotically stabilizing control, the Lyapunov rate in Eq. 19 is set equal to $-[P]\dot{\Delta}\rho$. The resulting control is obtained by using the least-squares inverse of the control effects matrix.

$$\boldsymbol{u} = -[B]^T([B][B]^T)^{-1}\left([P](\dot{\boldsymbol{\delta\rho}}) + \boldsymbol{f}(\boldsymbol{\delta\rho}) + \boldsymbol{\delta a}_{\mathrm{C}} + \boldsymbol{\delta a}_{\mathrm{D}} - \ddot{\boldsymbol{\rho}}_{\mathrm{r}} + \dot{\boldsymbol{f}}(\boldsymbol{\delta\rho}, \dot{\boldsymbol{\delta\rho}})\right) \tag{23}$$

RESULTS

A scenario is simulated in which the two craft approach in the along-track (HCW-Y) direction. Electrostatic actuation is used to place the follower at the nominal HCW state of $[0,-1,0,0,0,0]^T$. It is assumed that the follower remains within the plasma wake at all times. Two separate initial conditions are considered, both of which use the HCW STM to place the follower at a nominal position of [-0.1 m, -1 m, 0 m, 0 m/s, 0 m/s, 0 m/s]^T. The control corrects the offsets from the nominal position. The first scenario places the follower at the off-nominal position after a quarter orbit while the second uses a half orbit. See the spacecraft parameters for both simulations displayed in Table 1. Note that in both simulations, Solar Radiation Pressure (SRP) and J_2 are included as unmodeled perturbations.

The same circular, equatorial orbit is used for both simulations with semi-major axis of 7×10^7 m. Finally, after tuning the gains in Eq. (23), the same set was determined to perform best for both simulations. These are given in table 2.

Parameter	Leader	Follower
Number of Charged Spheres	10	1
Charged Sphere Radius (m)	0.25	0.25
Charge Structure Radius (m)	0.5	N/A
Mass (kg)	1000	1
Drag Coefficient	2.2	2.2
Reflectivity Coefficient	2	2
Cross-Sectional Area (m^2)	3.1415	0.0314

Table 1. Spacecraft Parameters

Parameter	Value
K	0.001
P	0.05
$\dot{\delta\rho}_{\max}$	0.001 m/s

Table 2. Gains used in scenario 1

Scenario 1

The initial HCW state of the follower — which would arrive at the off-nominal position after a quarter period given only HCW dynamics — is [-0.4000 m, -1.3425 m, 0 m, 0.0003 m/s, 0.0006 m/s, 0 m/s]^T. The difference between the true and reference HCW states is displayed in Figure 2.

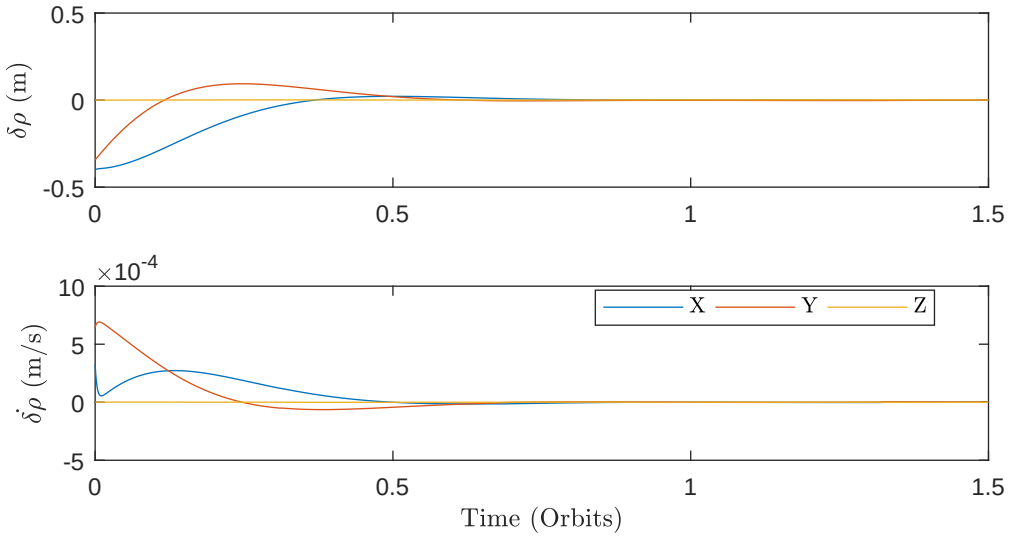

Figure 2. Deviation of HCW position and velocity relative to nominal for scenario 1

Note that the system does not settle to the nominal position in a quarter period, even though the initial conditions were intended to place the follower very near that position after that amount of time. This is because the gains and saturated position control are set such that reasonable voltages are sourced. These voltages are displayed in Figure 3.

Initially, large voltages are sourced to influence the trajectory of the follower toward the nominal state. After this, voltages are bounded by ± 400 V. These voltages could likely be sourced by a spacecraft power

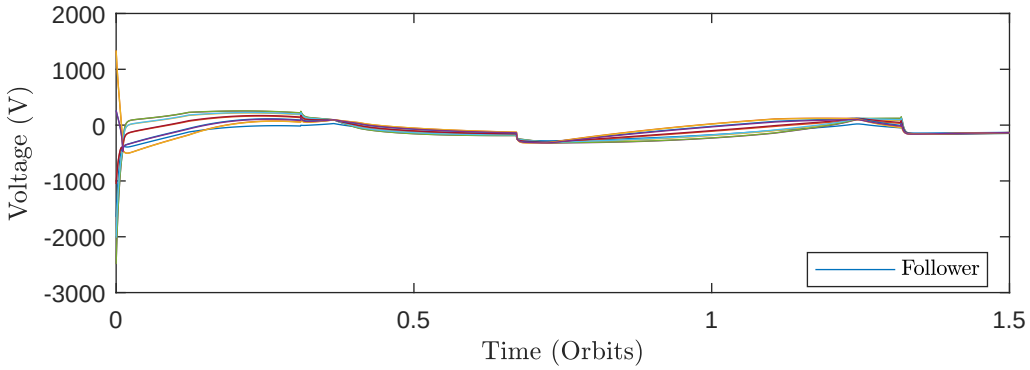

Figure 3. Control voltages for scenario 1

system, though the complicated wake dynamics and dependence on system geometry and the leader and follower craft sizes makes solid conclusions difficult. Relative to previous investigations, these control voltages are much lower, indicating that this control methodology could prove successful or future applications.

The initial control spike followed by a region of bounded voltages demonstrates the reliance of the control methodology on trajectory design. An improved trajectory could decrease the total control usage. As this investigation considers only control methods, careful trajectory selection is out of scope. The steps in the control voltages are due to the spacecraft passing in and out of eclipse and the resulting changes in drag and SRP.

Given that rendezvous are typically considered in terms of matching orbits rather than simply achieving proper relative positions, the time evolution of the difference between the leader's and follower's semi-major axis and eccentricity is included. Figure 4 shows only the two aforementioned elements because the orbits are designed such that they are initially co-planar.

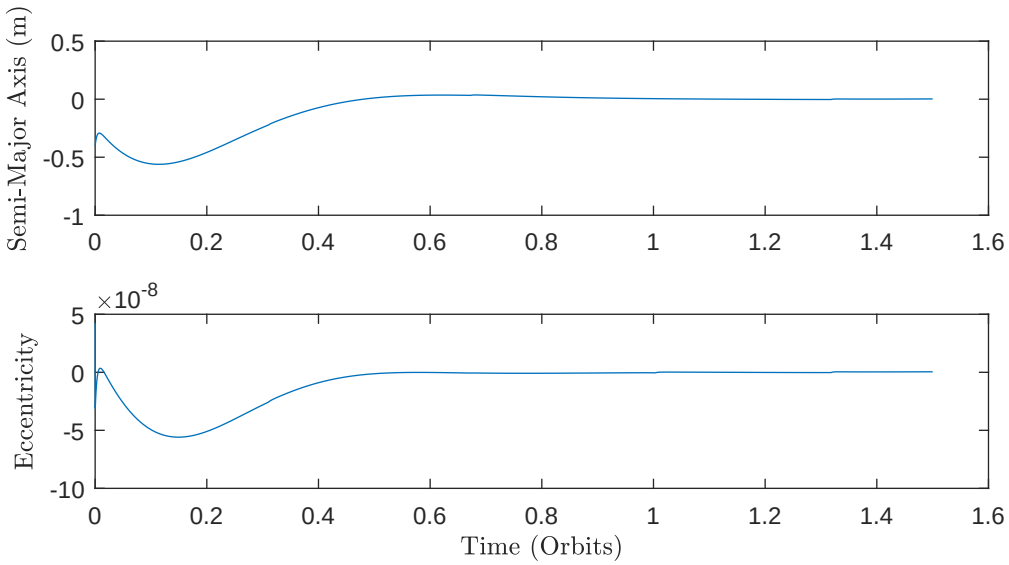

Figure 4. Difference in orbit shape between leader and follower for scenario 1

Scenario 2

The second scenario is initiated with follower HCW state [-0.7000 m, -2.8850 m, 0 m, 0 m/s, 0.0013 m/s, 0 m/s]^T. Note that the difference between the follower HCW state and the nominal shown in Figure 5 again settles well after the intended time. Larger deviations are seen relative to Figure 2 because the initial offset is larger.

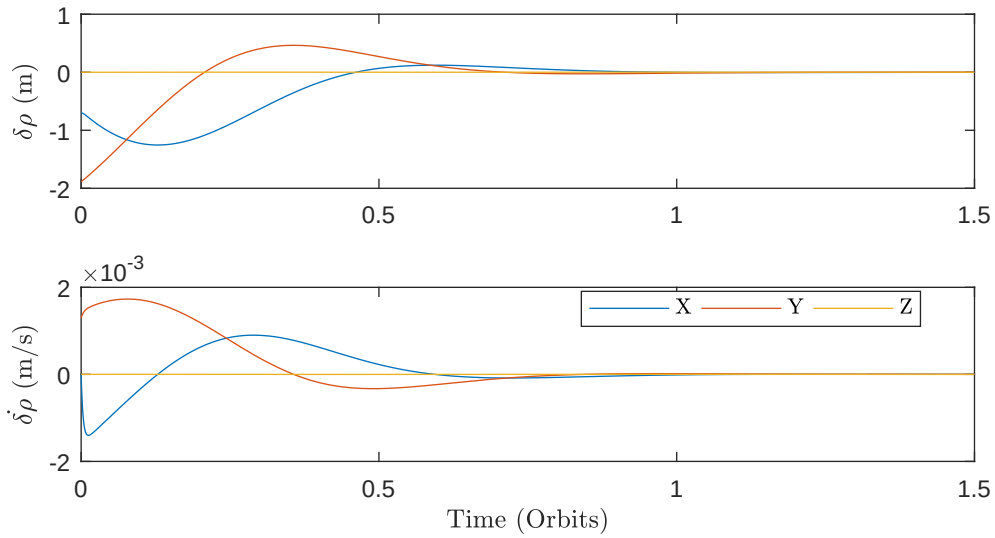

Figure 5. Deviation of HCW position and velocity relative to nominal for scenario 1

The control voltages shown in Figure 6 are much larger than in the previous scenario. It is unlikely that spacecraft power systems could source voltages of this magnitude, given that a collapse of the wake — resulting from the streaming ions being attracted down onto the negatively charged spheres — would cause a massive increase in power. While the position control loop saturates, the velocity is not throttled and the relative velocities in this later simulation are much larger.

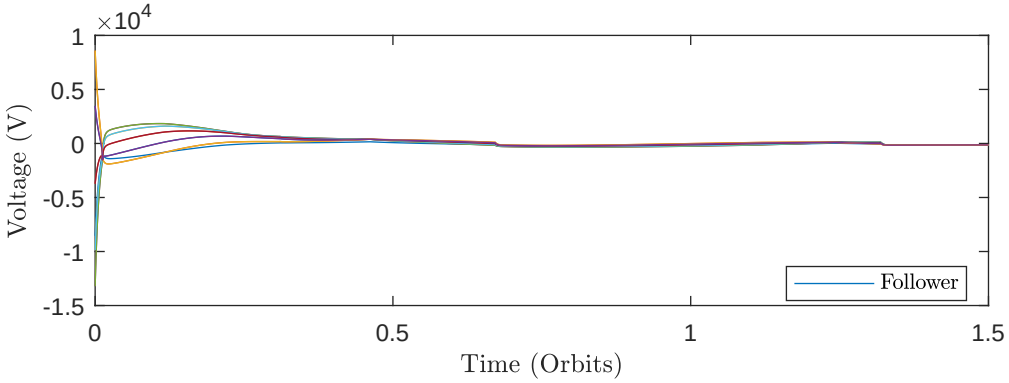

Figure 6. Control voltages for scenario 1

Again for completeness, the orbit elements of the follower relative to the leader are provided. Figure 7 demonstrates behavior similar to Figure 4 on timescales similar to Figure 5.

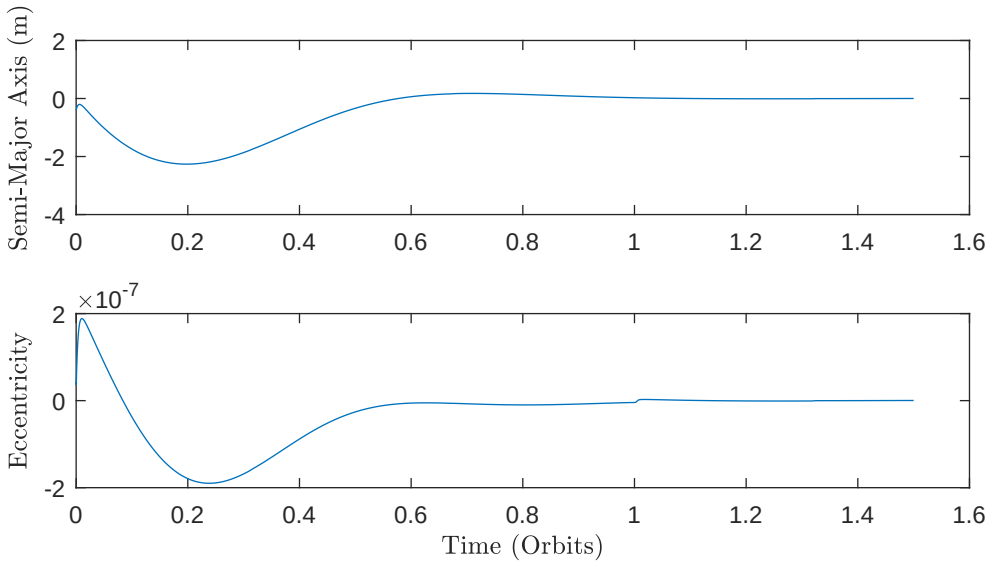

Figure 7. Difference in orbit shape between leader and follower for scenario 2

CONCLUSION

A charge-product based nonlinear controller is developed for an electrostatic actuation system using Lyapunov Direct Method. Two separate initial conditions are considered and the control effort required to achieve a nominal position demonstrates the techniques reliance on trajectory design. Future work will consider both improvements in control methodology and trajectory design.

The results presented indicate that, given proper use of the derived control, rendezvous operations can be achieved with relatively low control usage given that the chaser craft is placed within the wake of the target.

REFERENCES

[1] Wigbert Fehse. *Automated rendezvous and docking of spacecraft*, volume 16. Cambridge university press, 2003.
[2] Lb King and Gg Parker. Spacecraft formation-flying using inter-vehicle coulomb forces. *NASA Institute for . . .*, pages 1–103, 2002.
[3] Trevor Bennett, Daan Stevenson, Erik Hogan, and Hanspeter Schaub. Prospects and challenges of touchless electrostatic detumbling of small bodies. *Advances in Space Research*, 56(3):557–568, 2014.
[4] Hanspeter Schaub and Zoltán Sternovsky. Active space debris charging for contactless electrostatic disposal maneuvers. *Advances in Space Research*, 53:110–118, 2014.
[5] Erik A. Hogan and Hanspeter Schaub. Impacts of tug and debris sizes on electrostatic tractor charging performance. *Advances in Space Research*, 55(2):630–638, 2015.
[6] Erik A. Hogan and Hanspeter Schaub. General High-Altitude Orbit Corrections Using Electrostatic Tugging with Charge Control. *Journal of Guidance, Control, and Dynamics*, 38(4):699–705, 2015.
[7] Laura A. Stiles, Hanspeter Schaub, Kurt K. Maute, and Daniel F. Moorer. Electrostatically inflated gossamer space structure voltage requirements due to orbital perturbations. *Acta Astronautica*, 84:109–121, 2013.
[8] D E Hastings. A review of plasma interactions with spacecraft in low Earth orbit. *Journal of Geophysical Research*, 100(A8):14457–14483, 1995.
[9] William B Smythe. Static and dynamic electricity. 1988.
[10] Hanspeter Schaub and Scott Piggott. Speed-constrained three-axes attitude control using kinematic steering. *Acta Astronautica*, 147:1–8, 2018.